JOURNAL of
MATERIALS and MECHATRONICS:A

e-ISSN 2717-8811
JournalMM, 2024, 5(2), 341-353
https://doi.org/10.55546/jmm.1576256

Araştırma Makalesi / Research Article

Effect of Graphene Reinforcement on Boronization in FeCo Medium Entropy Alloys Produced by Different Methods

Nazmiye Nur KÜÇÜKELÇİ[1],Ersan MERTGENÇ[2*], Rıza KARA[3]

[1] Afyon Kocatepe University, Institute of Science, Department of Nanoscience and Nanotechnology, Afyonkarahisar, Türkiye,
ORCID ID: https://orcid.org/0000-0003-4937-6626, nkelci@hotmail.com
[2*] Afyon Kocatepe University, Afyon Vocational High School, Department of Railway Systems, Afyonkarahisar, Türkiye,
ORCID ID: https://orcid.org/0000-0001-8247-2922, ersanmertgenc@hotmail.com
[3] Usak University, Vocational School of Technical Sciences, Faculty of Technology, Department of Mechanical and Metal Technologies, Usak, Türkiye,
ORCID ID: https://orcid.org/0000-0002-0820-2577, riza.kara@usak.edu.tr

Geliş/ Received: 30.10.2024**;** **Revize/Revised:** 24.11.2024 **Kabul / Accepted:** 03.12.2024

ABSTRACT: With the developing technology, studies on the production and development of new materials are intensifying as traditional materials are inadequate to meet the needs of the industry. As an alternative to traditional steels, the use of low, medium and high entropy alloys and nanomaterials has recently become one of the most suitable solutions. Based on these solutions, in this study; the effect of nanoparticle reinforcement material on the boride layer structure in pack boriding of FeCo alloy, which is described as a soft magnetic alloy and produced by different methods, was investigated. Firstly, 2% and 4% graphene reinforced, medium entropy FeCo alloy was produced by 2 different methods melt casting (MC) and powder metallurgy (PM). Then, medium entropy alloys (MEAs) produced by both methods were subjected to a pack boronizing process at 1073 K temperature for 2 hours. Both the produced MEAs and the boride layers of the borided MEAs were characterized. When the microstructures of the produced alloys are examined, it is seen that with the increase in graphene reinforcement, the tendency for dendritic structure increases in alloys using the MC method, while crack formation increases in alloys using the PM method. According to the XRD pattern analysis of the alloys produced by both methods, peaks belonging to the CoFe phase were detected in the main peaks of the alloys. The microhardness of the alloys ranges between 258 $HV_{0.05}$ and 314 $HV_{0.05}$. In the boride layer structures obtained by pack boronizing, no transition zone is formed, they are columnar and have a sawtooth appearance. Boride layer thicknesses range between 22 µm and 34 µm. According to the XRD pattern analysis of the boride layers of the alloys produced by both methods, FeB, Fe_2B, CoFe phases were detected in the main peaks, while the Co_2Fe phase was also present in the alloys produced by the MC method. The surface microhardness of the boride layers varies between 1922 $HV_{0.05}$ and 2124 $HV_{0.05}$.

Keywords: Medium entropy alloy, Graphene, Melt casting, Powder metallurgy, Pack boriding

*Sorumlu yazar / Corresponding author: ersanmertgenc@hotmail.com
Bu makaleye atıf yapmak için /To cite this article

Küçükelçi, N. N., Mertgenç, E., Kara, R. (2024). Effect of Graphene Reinforcement on Boronization in FeCo Medium Entropy Alloys Produced by Different Methods. Journal of Materials and Mechatronics: A (JournalMM), 5(2), 341-353.

1. INTRODUCTION

With the rapid development of technology in recent years, traditional commercial materials may be inadequate to meet the needs of the industry. In order to provide the expected properties, intensive studies are being carried out by researchers to develop different alloys. Especially high entropy alloys (HEA), medium entropy alloys (MEA) and low entropy alloys (LEA) are among the leading solutions in obtaining the desired properties in recent years.

Entropy, in physics, refers to the thermal energy of a system that cannot be converted into mechanical work. It is defined as disorder and randomness in the system. In the literature, the concept of entropy is divided into 2 classes. It is defined as alloys consisting of at least five elements and their concentrations are between 5% and 35% On the other hand, according to the entropy-based definition, it is examined in 3 classes as low, medium and high entropy alloys according to the amount of elements they contain. When determining the class to which the alloy belongs, calculations are made according to the configuration entropy; alloys formed up to 2 elements are called low entropy, alloys containing 3 and 4 elements are called medium entropy, and alloys containing 5 and more elements are called high entropy.

Magnetic materials constitute a significant portion of engineering alloys. Among commercial magnetic materials, FeCo alloys are considered to have the highest saturation. These alloys are soft magnetic materials and are used in high temperature applications because they have low coercivity, high Curie temperature and high magnetization (Küçükilhan et al., 2024; Yu et al., 1999). In the production of alloys, melting and powder metallurgy methods are mostly preferred.

In cases where alloys are exposed to wear or work in corrosive environments, surface coating applications are also carried out as in conventional steels. The most common surface coating methods used are laser coatings (Riquelme & Rodrigo, 2021) aluminization (Bölükbaşı et al., 2023), atmospheric plasma spray (APS) (Michalak et al., 2021), electro spark deposition (Padgurskas et al., 2017), high-velocity oxygen fuel injection (HVOF) (Pulido-González et al., 2020) and boronization (Elias-Espinosa et al., 2015; Mishigdorzhiyn et al., 2020).

Boriding is based on the formation of a hard boride layer on the surface depending on the chemical composition of the substrate material in liquid, solid and gas environments. The process is a thermochemical method based on diffusion performed at high temperatures. Therefore, the boride layer formed on the surface of the material has low roughness, is solid and permanent. The pack-boriding method is widely used due to its easy applicability and economic operation. The process can be performed in a wide range of temperatures ranging from 973 K to 1273 K and durations of 1-10 hours.

According to literature research; There are quite a few studies on the production method and magnetic properties of FeCo alloy. However, studies on the effect of nanoparticle reinforcement elements on the alloy system and the effects of reinforcement elements on surface coatings are quite limited in these alloys. In this study, the manufacturability of FeCo alloy was investigated using MC and PM methods. In addition, different amounts of graphene reinforcement were added to FeCo alloys produced with different methods. The effect of graphene on the boride layer to be formed on the alloys was examined in detail using the pack-boriding method of FeCo alloys containing different amounts of graphene reinforcement.

2. MATERIALS AND METHODS

In this study, iron (Fe) and cobalt (Co) powders with a size of -325 mesh and graphene (G) powder with a size of 3 nm supplied by Nanografi company were used. The chemical equivalents of the Fe/Co alloy used are given in Table 1, and the powder mixing ratios of the prepared MEAs are given in Table 2.

Table 1. Information on Fe/Co alloy

Element	Atomic weight (u)	Mixing ratio (%wt)	Mixing ratio (%at)
Fe	55.845	50	51.3444
Co	58.933	50	48.6556

Table 2. MEA codes, production methods and mixing ratios

Alloy code	Production method	Graphene (%)	Fe (g)	Co (g)	Graphene (g)	Total (g)
MC-0	Melt Casting	0	5.00	5.00	-	10.00
MC-2	Melt Casting	2	4.90	4.90	0.20	10.00
MC-4	Melt Casting	4	4.80	4.80	0.40	10.00
PM-0	Powder Metallurgy	0	5.00	5.00	-	10.00
PM-2	Powder Metallurgy	2	4.90	4.90	0.20	10.00
PM-4	Powder Metallurgy	4	4.80	4.80	0.40	10.00

A lathe machine was used to mix the powders whose compositions were determined and weighed, and they were mixed at 120 rpm for 12 hours. A Seles brand JTA model scale with a 0.001 gr sensitivity was used to weigh the powders. The powders, which were mixed and made homogeneous, were pressed in a Ø20 mm diameter mold, with a single-axis press at 400 bar pressure, and turned into cylindrical pellets for powder metallurgy and melt casting.

The alloys to be produced with the powder metallurgy method were sintered for 1 hour at 1273 K in a protective gas atmosphere and made ready for boronization. In the alloys to be produced with the melt casting method, pellets shaped in the press were used. Two molds were designed for the melting process; the first was used for the master alloy production and the second was used for the final alloy production. In the master alloy production, the alloys were turned upside down in each melting process and melting was done 4 times and all processes were carried out in an argon protective gas atmosphere. In the mold used in the production of the final alloy, a reverse vacuum system was used and when the alloy reached the liquid phase during melting, the air previously collected in the air accumulator chamber with a vacuum pump was drawn (-0.1 atm) to produce the final alloy. In the production of the alloys, a Welder TIG 400 DC pulse model TIG welding machine was used at 210 A. The copper melting molds used for the production of the alloys is given in Figure 1(a) and the alloy production system is given in Figure 1(b).

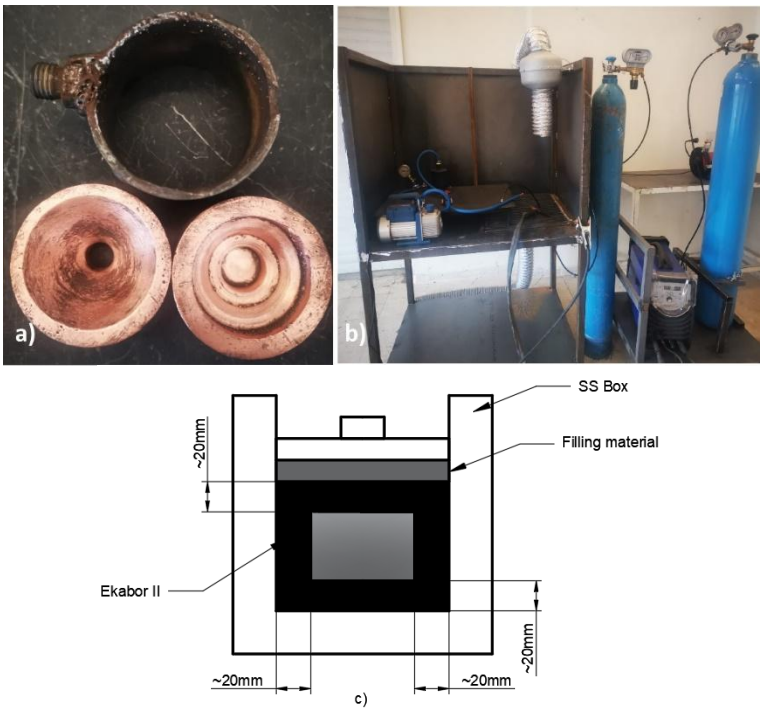

Figure 1. a) Copper mold and b) production system used in the MC process c) Schematic view of the pack-boronizing method

Boriding of alloys produced by MC and PM methods was carried out in a chamber type furnace with commercial Ekabor II (90% SiC, 5% B_4C and 5% KBF_4) coating powder environment at 1073 K for 2 hours by package boronizing method. Alloys to be coated were placed in Ekabor II powder in the center of the box made of stainless steel (at least 20 mm distance from the box edges).

For microstructural examination of boronized and non-boronized alloys, non-boronized alloys were prepared metallographically and SEM analyses were performed by LEO 1430VP brand SEM imaging, SEM analyses of boronized alloys were performed without metallographic preparation. X-ray diffraction analysis using CuKα (α= 1.5406˚A) radiation, Shimadzu XRD-6000 brand X-ray diffractometer and microhardness measurements were performed at three separate points at 10 μm intervals under a 50 g load for 15 seconds, Shimadzu HMV-2L model microhardness measuring device were used. The flow chart of this study is given in Figure 2.

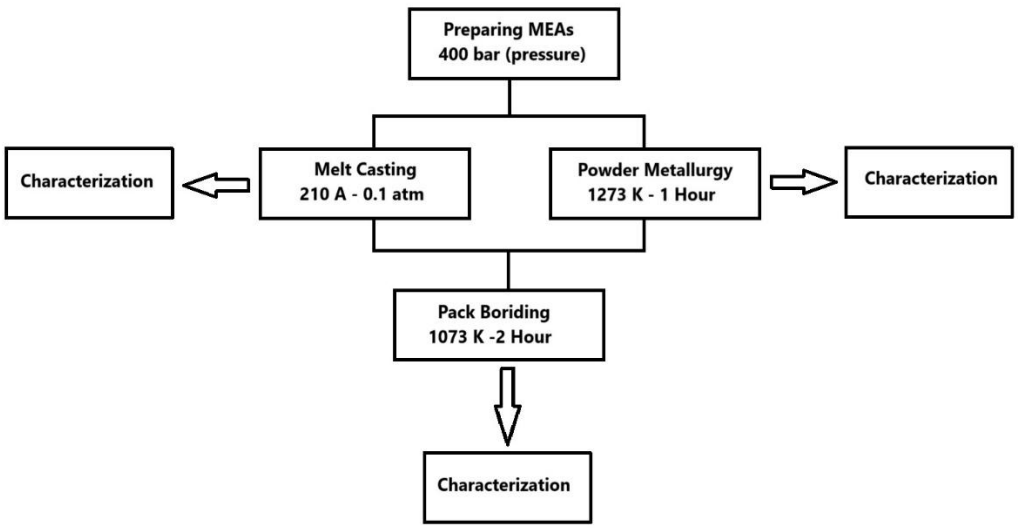

Figure 2. Flow chart of the study

3. RESULTS AND DISCUSSION

3.1 Characterization of MEAs

In Figure 3, SEM (backscatter electrons) microstructure images of unreinforced, 2% and 4% graphene reinforced alloys produced by melt casting (MC) and powder metallurgy methods (PM) are given together with EDS elemental analysis.

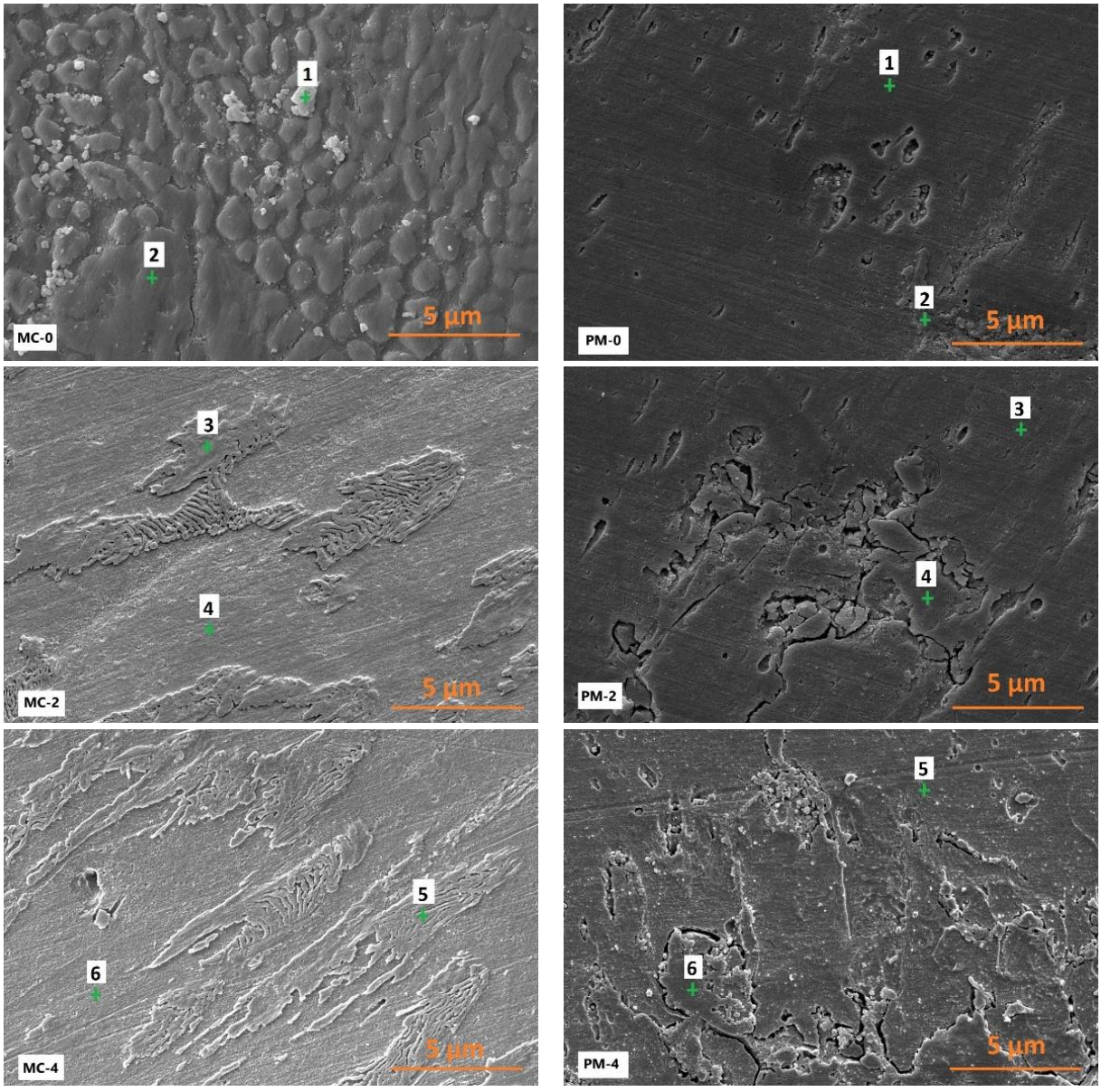

MC

Point	Fe (%)	Co (%)	C (%)	Al (%)	O (%)
1	11.73	9.35	--	52.41	23.36
2	49.78	45.96	--	--	4.26
3	48.92	43.79	2.87	1.04	3.38
4	45.42	48.28	1.71	0.46	4.13
5	49.82	39.23	5.14	0.75	5.06
6	42.44	50.25	3.07	0.22	4.02

PM

Point	Fe (%)	Co (%)	C (%)	Al (%)	O (%)
1	46.73	50.75	--	0.28	2.24
2	48.64	43.92	--	2.02	5.42
3	47.68	49.78	1.14	0.44	0.96
4	52.12	37,70	2.92	3.14	4.12
5	45.64	46.76	3.56	0.32	3.72
6	47.84	34.14	5.02	4.26	8.74

Figure 3. MEAs, SEM(BE) microstructure and EDS point analyses (%wt)

When the microstructures of the samples produced by the melt casting and powder metallurgy methods are examined together, the microstructure of those produced by the casting method has a multiphase structure, while the single-phase structure is dominant in the production with powder metallurgy. In the production with melt casting, due to the unstable solidification of alloy elements with different melting temperatures in the system with graphene reinforcement, the matrix structure tends to form dendritic (Li et al., 2022). In powder metallurgy production, an increase in inclusions and cracks is observed with the increase in the amount of graphene reinforcement. This situation is attributed to the fact that the alloy elements in the system have different thermal properties and that there are weak bonds on the surfaces (Zhu et al, 2023). On the other hand, according to the EDS elemental analyses in production with both methods, the Fe and Co ratios are approximately at the production amounts, and the C amount increases with graphene reinforcement. In addition, according to elemental analysis, the dendritic parts formed in production by arc melting are carbon-rich regions. Although the melting process is carried out in a protective gas (argon) atmosphere, since there is no vacuum system, there is oxygen in the structure, albeit in low amounts. The increase in oxygen amounts in carbon-rich dendritic regions is due to the increase in the melting temperature of carbon during melting. The fact that the amount of aluminum is high (in the elemental analysis of MC-0 sample) along with oxygen at point number 1 shows that this grain is not due to production, but rather due to alumina suspension during polishing at the sample preparation stage. The amount of oxygen in production with powder metallurgy is higher than in production with melt casting. The biggest disadvantage of production with powder metallurgy method is that the oxide phases formed in the material cannot be removed due to their stable structure and do not decompose easily. Therefore, even if protective gas is used both during production and sintering, if the temperature does not reach a sufficient value, the oxides continue to exist in the structure, albeit partially (Fang et al., 2018).

Figure 4 shows the XRD pattern analysis of the unreinforced and graphene reinforced MEA produced by MC (Figure 4a) and PM (Figure 4b) methods.

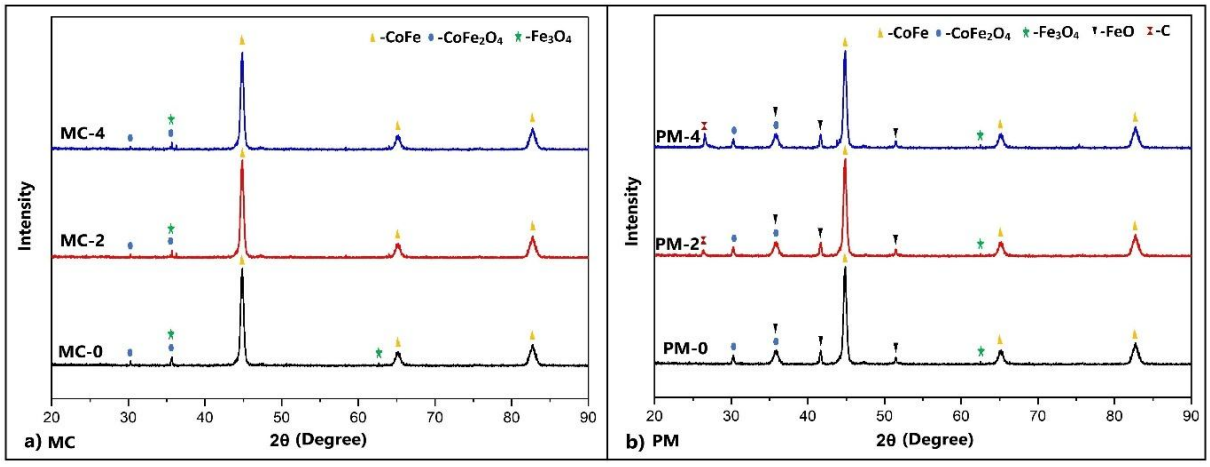

Figure 4. XRD pattern analysis of unreinforced and graphene reinforced MEAs a) melt casting, b) Powder Metallurgy

CoFe (PDF: 01-071-5029) phase with a single-phase solution crystal structure and a body-centered cubic (BCC) structure is located in the main peaks. In the secondary peaks, there are peaks belonging to the oxide phases $CoFe_2O_4$ (PDF: 01.074.6403) and Fe_3O_4 (PDF: 00-026-1136) due to Fe and Co (Allaedini et al., 2015; Gill et al., 2019). In the MEAs produced by powder metallurgy, the peaks belonging to the FeO (PDF: 00-006-0615) phase and the C (graphite) (PDF: 00-056-0159) phase become more pronounced, and the volume of these phases increases with the increase in the

amount of graphene reinforcement. This result is also consistent with the EDS analysis in Figure 3. While the C peak is not present in the productions made with the melt casting method, its presence in the productions made with powder metallurgy can be attributed to the insufficient sintering temperature or time. The increase in the peaks of oxide phases in production by powder metallurgy method is due to insufficient protective gas environment or temperature (Tan et al., 2021).

Figure 5 shows the graph of microhardness values of MEA alloys.

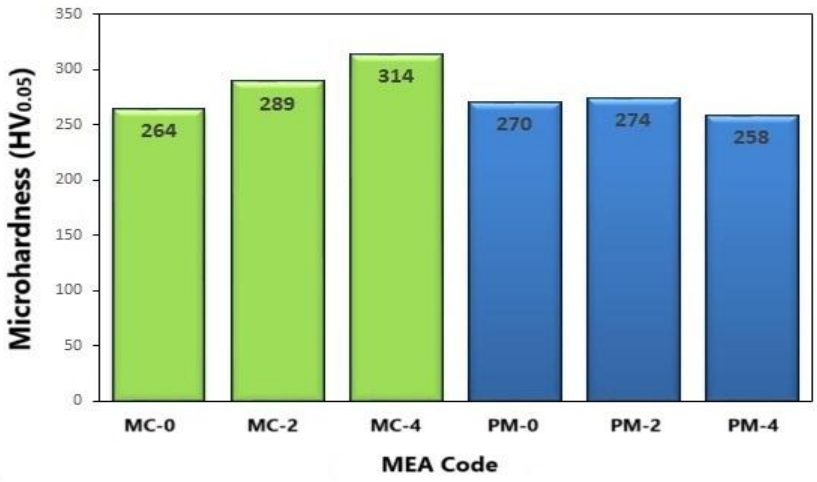

Figure 5. Microhardness of MEAs

The microhardness values of the graphene unreinforced alloys (MC-0 and PM-0) were measured as 264 $HV_{0.05}$ - 270 $HV_{0.05}$. 2% and 4% graphene reinforced alloys (MC-2, MC-4, PM-2 and PM-4) MEAs produced by MC and PM methods were measured as 289 $HV_{0.05}$ - 274 $HV_{0.05}$ and 314 $HV_{0.05}$ - 258 $HV_{0.05}$, respectively. In literature studies on FeCo alloys, it has been recorded that hardness values are evaluated between 235 HV and 314 HV (Albaaji et al., 2017; Mani et al., 2014). It has been recorded in the literature that graphene reinforcement to different alloys causes an increase in properties such as hardness, density, corrosion and wear resistance of the alloys (Liang et al., 2025; Zhang et al., 2022). In samples produced with the melt casting method, microhardness values also increase with the increase in the reinforcement ratio. It is thought that this situation is due to the more homogeneous distribution of the carbon element in the alloy system by using the melt casting method. On the other hand, in the samples produced with the powder metallurgy method, although the hardness values were close to each other, there was no stable change depending on the reinforcement ratio. As can be seen in the SEM images of the samples produced with powder metallurgy (Figure 3), there are cracks in the samples with graphene reinforcement and their distribution is irregular. The instability of the measurement values may be due to phase differences at the points where the hardness values are measured and discontinuities such as porosity, precipitation and cracks.

3.1 Characterization of Boride Layers

Figure 6 shows the SEM microstructure images of the boride layers of unreinforced, 2% and 4% graphene reinforced FeCo alloy produced by melt casting and powder metallurgy methods, which were boronized at 1073 K for 2 hours, and Figure 7 shows the graph of boride layer thicknesses.

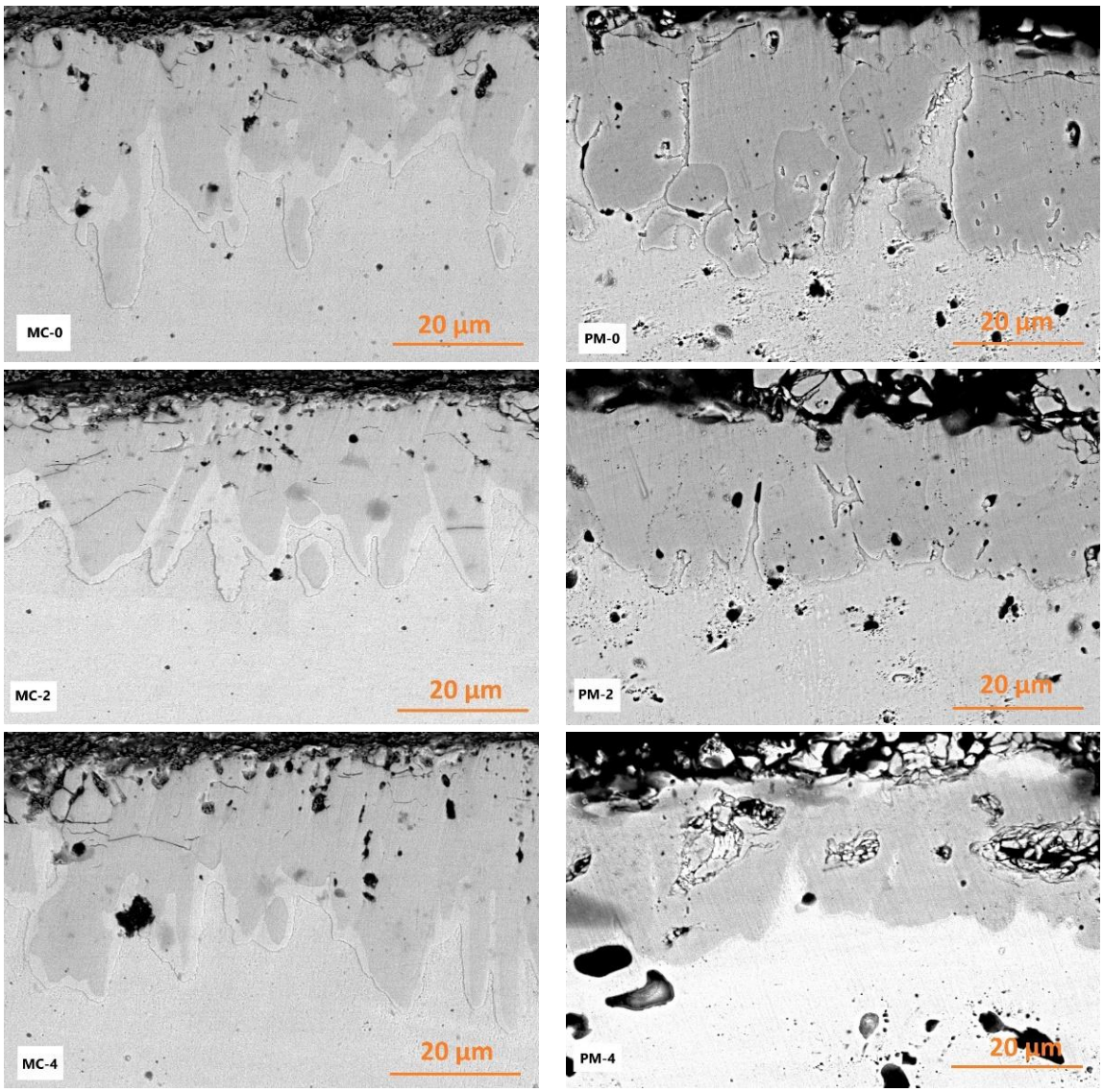

Figure 6. SEM (BE) images of boron layer of unreinforced and graphene reinforced MEAs

When the boride layer structures of MEAs produced by melt casting and powder metallurgy methods are examined, it is seen that no transition region is formed and the boride layers are columnar and have a sawtooth appearance.

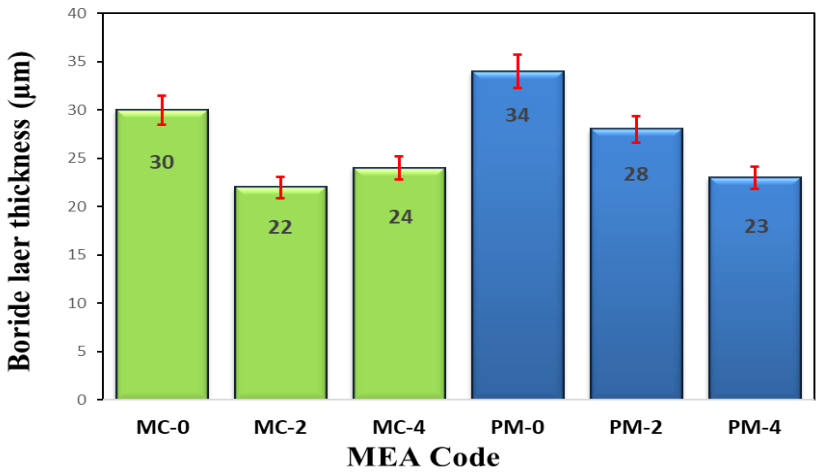

Figure 7. Boride layer thicknesses of unreinforced, 2% and 4% graphene reinforced MEAs

In the boriding of unreinforced, 2% and 4% graphene reinforced FeCo alloy produced using melt casting and powder metallurgy methods at 1073 K for 2 hours, the boride layer thicknesses were obtained as 30 µm - 34 µm, 22 µm - 28 µm and 24 µm - 23 µm, respectively. The formation of a thicker boride layer in unreinforced alloys is thought to be due to the absence of graphene reinforcement in these alloys and the interstitial atom behavior of boron atoms allowing them to diffuse to longer distances without any carbon element barrier.

When the microstructure images in Figure 6 is evaluated together with the boride layer thicknesses in Figure 7; it is seen that the boride layer thicknesses decrease as the amount of graphene reinforcement increases. It can be thought that as the amount of the element in the alloy increases, the boron element strengthens the diffusion to enter deeper distances. (Gao et al., 2022; Mertgenç and Kayali, 2022). Again, as the amount and ratio of alloying elements increase, the cracks in the boride layer increase, their lengths tend to extend, and fractures occur in the boride layer. This is due to the different thermal expansion properties of the alloy elements with different properties in the system (Cengiz, 2021).

Figure 8 shows the XRD pattern analysis taken from the boride layer surface of unreinforced, 2% and 4% graphene reinforced MEAs produced by melt casting and powder metallurgy methods, after boronizing at 1073 K for 2 hours.

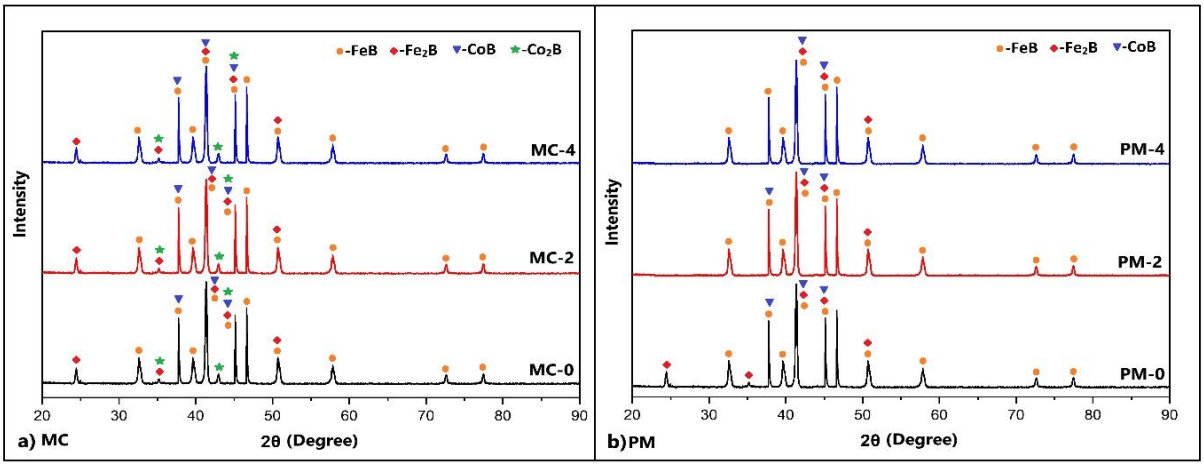

Figure 8. XRD pattern analysis of boride layer of MEAs a) Melt casting, b) Powder Metallurgy method

According to the XRD pattern analyses there are peaks belonging to the FeB (PDF: 03-065-2599), Fe_2B (PDF: 01-072-1301), CoB (PDF: 03-065-2596) phases in the main peaks of the boride layers (Alkan, 2023). While there are also low amounts of Co_2B (PDF: 03-065-2962) phase peaks in MEAs produced by the casting method, peaks belonging to this phase cannot be found in MEAs produced by the PM method. In addition, in the boronization of alloys produced by PM, the Fe_2B phase decreases in volume as the reinforcement ratio increases compared to the alloy without graphene reinforcement. In the microstructure images of the coated MEAs (Figure 6, Figure 7), it can be seen that the coating layers of the samples produced by PM are composed of similar phases compared to those produced by the casting method. This supports the absence of the Co_2B phase in the samples produced by powder metallurgy and the decrease in volume of the Fe_2B phase. On the other hand, cobalt and iron, which are the main elements that make up MEA, have very close atomic radii (r_{Co} = 0.125 nm, r_{Fe} = 0.126 nm). Therefore, they have a high solid solution degree with each other in iron and cobalt alloys (Wang et al., 2021) and it is very difficult to separate the two elements from each other in these systems.

Figure 9 shows the graph of microhardness values taken from the surface towards the matrix of unreinforced and graphene reinforced MEAs with different ratios produced by melt casting and powder metallurgy methods, after boronizing at 1073 K for 2 hours.

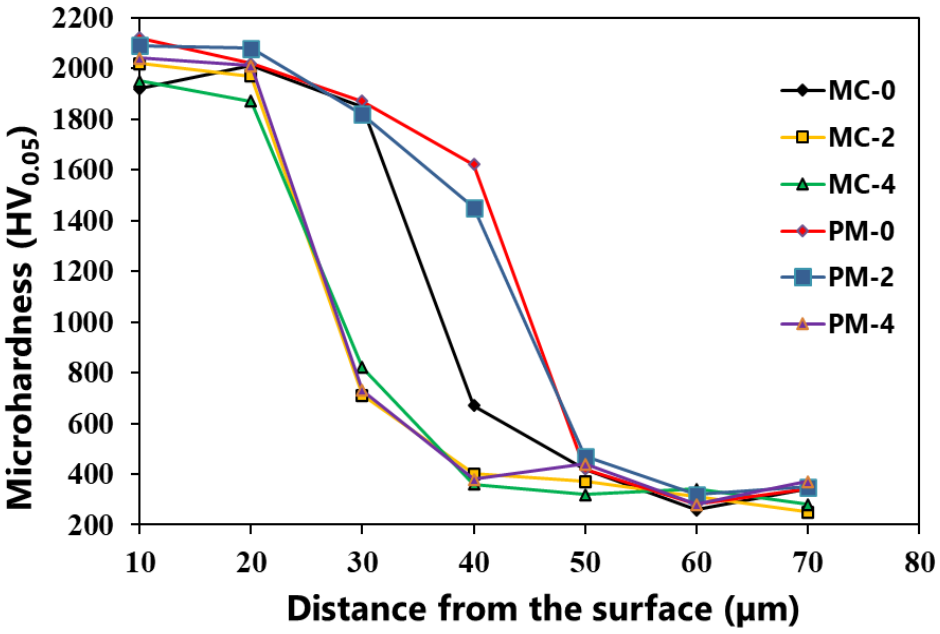

Figure 9. Microhardness graph of boride layers of MEAs

When Figure 9 is examined, the borided surface hardness of the MC-0, MC-2 and MC-4 alloys produced by the casting method were measured as 1922 $HV_{0.05}$, 2018 $HV_{0.05}$ and 1956 $HV_{0.05}$, respectively, and the surface hardness of the PM-0, PM-2 and PM-4 alloys produced by the powder metallurgy method were measured as 2124 $HV_{0.05}$, 2086 $HV_{0.05}$ and 2040 $HV_{0.05}$, respectively. In the literature, it has been recorded that in previous studies conducted on the surfaces of different materials by pack boronizing, the hardness of the FeB phase obtained is around 2350 HV (Kulka et al., 2017), the hardness of the CoB phase is between 2200 HV and 2753 HV (Campos-Silva et al., 2013; Rodríguez-Castro et al., 2015), the hardness of the Fe_2B phase is between 1748 HV and 1866 HV (Kulka et al., 2017), and the hardness of the Co_2B phase is around 1835 HV (Campos-Silva et al., 2013). So, in the present study, the measured boride layer surface hardnesses are compatible with the literature.

4. CONCLUSION

The results obtained in the investigation of the production of FeCo alloys produced without reinforcement, with 2% and 4% graphene reinforcement by melt casting and powder metallurgy methods and their boronization at 1073 K for 2 hours using the pack boronizing method are given below;

- While the microstructures of the alloy produced with the PM method graphene unreinforcement (PM-0) consist of a single phase, it was observed that the microstructure of the alloy produced with the MC method graphene unreinforcement (MC-0) consists of a double phase. With the increase in the graphene reinforcement ratio, the tendency for dentritic

structure in MEAs produced by the melt casting method increases, while cracks and porosities increase in MEAs produced by the powder metallurgy method.

- Peaks belonging to CoFe, $CoFe_2O_4$ and Fe_3O_4 phases were detected in alloys produced by the melt casting method, while peaks belonging to CoFe, $CoFe_2O_4$, Fe_3O_4, FeO and C phases were detected in alloys produced by the powder metallurgy method.
- The microhardness of unreinforced and graphene reinforced MEAs varies between 264 $HV_{0,05}$ and 314 $HV_{0,05}$.
- The boride layers of MEAs produced by both methods and boronized at 1073 K for 2 hours are columnar and have a sawtooth appearance.
- The boride layer thicknesses of the MEAs produced by the melt casting method and boronized were 30 μm in the unreinforced alloy, 22 μm in the 2% graphene reinforced alloy, and 24 μm in the 4% graphene reinforced alloy. The boride layer thicknesses of the MEAs produced by the powder metallurgy method were 34 μm in the unreinforced alloy, 28 μm in the 2% graphene reinforced alloy, and 23 μm in the 4% graphene reinforced alloy.
- Peaks belonging to FeB, Fe_2B, CoB and Co_2B phases were detected on the boride layer surfaces of MEAs produced by the melt casting method, and peaks belonging to FeB, Fe_2B and CoB phases were detected on the boride layers of MEAs produced by the powder metallurgy method.
- The boride layer hardnesses of the reinforced and graphene reinforced MEAs ranged between 1922 $HV_{0.05}$ and 2086 $HV_{0.05}$, and the surface hardnesses of the boronized alloys produced by both methods increased by 8 to 10 times.

5. ACKNOWLEDGEMENTS

This study was supported by Afyon Kocatepe University Scientific Research Projects Coordination Unit with Project number of 22.FEN. BİL.26.

6. CONFLICT OF INTEREST

Authors approve that to the best of their knowledge, there is not any conflict of interest or common interest with an institution/organization or a person that may affect the review process of the paper.

7. AUTHOR CONTRIBUTION

Ersan MERTGENÇ contributed to the management of the concept and/or design process of the research, preparation of the manuscript, and final approval and full responsibility for the work. Rıza KARA contributed to the data analysis and interpretation of the results, as well as the critical analysis of the intellectual content. Nazmiye Nur KÜÇÜKELÇİ contributed to the data collection.

8. REFERENCES

Albaaji A. J., Castle E. G., Reece M. J., Hall J. P., Evans S. L., Effect of ball-milling time on mechanical and magnetic properties of carbon nanotube reinforced FeCo alloy composites. Materials and Design 122, 296-306, 2017. https://doi.org/10.1016/j.matdes.2017.02.091.

Allaedini G., Tasirin S. M., Aminayi P., Magnetic properties of cobalt ferrite synthesized by hydrothermal method. International Nano Letters 5(4), 183-186, 2015. https://doi.org/10.1007/s40089-015-0153-8.

Alkan S., Effect of Boron-Aluminide Coating Applied on R4 Grade Offshore Mooring Chain Steel on Pitting and Tribo-Corrosion Behaviour. Journal of Materials and Mechatronics: A 4(1), 302-317, 2023. https://doi.org/10.55546/jmm.1296633.

Bölükbaşı Ö. S., Serindağ T., Gürol U., Günen A., Çam G., Improving oxidation resistance of wire arc additive manufactured Inconel 625 Ni-based superalloy by pack aluminizing. CIRP Journal of Manufacturing Science and Technology 46, 89-97, 2023. https://doi.org/10.1016/j.cirpj.2023.07.011.

Campos-Silva I., Bravo-Bárcenas D., Meneses-Amador A., Ortiz-Dominguez M., Cimenoglu H., Figueroa-López U., Andraca-Adame J., Growth kinetics and mechanical properties of boride layers formed at the surface of the ASTM F-75 biomedical alloy. Surface and Coatings Technology 237, 402-414, 2013. https://doi.org/10.1016/j.surfcoat.2013.06.083.

Cengiz S., Effect of refractory elements on boronizing properties of the CoCrFeNi high entropy alloy. International Journal of Refractory Metals and Hard Materials, 95, 205418, 2021. https://doi.org/10.1016/j.ijrmhm.2020.105418.

Elias-Espinosa M., Ortiz-Domínguez M., Keddam M., Gómez-Vargas O. A., Arenas-Flores A., Barrientos-Hernández F. R., West A. R., Sinclair D. C., Boriding kinetics and mechanical behaviour of AISI O1 steel. Surface Engineering 31(8), 588-597, 2015. https://doi.org/10.1179/1743294415Y.0000000065.

Fang Z. Z., Paramore J. D., Sun P., Chandran K. S. R., Zhang Y., Xia Y., Cao F., Koopman M., Free M., Powder metallurgy of titanium–past, present, and future. International Materials Reviews 63(7), 407-459, 2018. https://doi.org/10.1080/09506608.2017.1366003.

Gao Z., Wang L., Wang Y., Lyu F., Zhan X., Crack defects and formation mechanism of FeCoCrNi high entropy alloy coating on TC4 titanium alloy prepared by laser cladding. Journal of Alloys and Compounds 903, 163905, 2022. https://doi.org/10.1016/j.jallcom.2022.163905.

Gill N., Sharma A. L., Gupta V., Tomar M., Pandey O. P., Singh D. P., Enhanced Microwave absorption and suppressed reflection of polypyrrole-cobalt ferrite-graphene nanocomposite in X-band. Journal of Alloys and Compounds, 797, 1190-1197, 2019. https://doi.org/10.1016/j.jallcom.2019.05.176.

Küçükilhan M., Mertgenç E., Çolak F., The effect of powder-pack aluminising on the corrosion performance of FeCoGx low entropy. International Journal of Surface Science and Engineering 18(3), 229-244, 2024. https://doi.org/10.1504/IJSURFSE.2024.141505.

Kulka M., Makuch N., Piasecki A., Nanomechanical characterization and fracture toughness of FeB and Fe2B iron borides produced by gas boriding of Armco iron. Surface and Coatings Technology, 325, 515-532, 2017. https://doi.org/10.1016/j.surfcoat.2017.07.020.

Li Y., Yang Z., Ma Z., Bai Y., Wu C., Li J., Effect of element V on the as-cast microstructure and mechanical properties of Al0.4Co0.5VxFeNi high entropy alloys. Journal of Alloys and Compounds 911, 165043, 2022. https://doi.org/10.1016/j.jallcom.2022.165043.

Liang L., Wu J., Wang B., Kong C., Pervikov A., Shi H., Li X., Microstructure and electromagnetic wave absorption properties of FeCo/graphene composites prepared by electrical wire explosion method. Applied Surface Science 681, 161577, 2025. https://doi.org/10.1016/j.apsusc.2024.161577.

Mani M. K., Viola G., Reece M. J., Hall J. P., Evans S. L., Influence of coated SiC particulates on the mechanical and magnetic behaviour of Fe-Co alloy composites. Journal of Materials Science 49(6), 2578-2587, 2014. https://doi.org/10.1007/s10853-013-7954-9.

Mertgenç E., Kayali Y., Diffusion kinetics and boronizing of high entropy alloy produced by TIG melting reverse suction method. Canadian Metallurgical Quarterly 62(2), 362-371, 2022. https://doi.org/10.1080/00084433.2022.2082203.

Michalak M., Sokołowski P., Szala M., Walczak M., Łatka L., Toma F. L., Björklund S., Wear behavior analysis of Al2O3 coatings manufactured by APS and HVOF spraying processes using powder and suspension feedstocks. Coatings 11(8), 879, 2021. https://doi.org/10.3390/coatings11080879.

Mishigdorzhiyn U., Chen Y., Ulakhanov N., Liang, H., Microstructure and wear behavior of tungsten hot-work steel after boriding and boroaluminizing. Lubricants 8(3), 26, 2020. https://doi.org/10.3390/lubricants8030026.

Padgurskas J., Kreivaitis R., Rukuiža R., Mihailov V., Agafii V., Kriūkienė R., Baltušnikas A., Tribological properties of coatings obtained by electro-spark alloying C45 steel surfaces. Surface and Coatings Technology 311, 90-97, 2017. https://doi.org/10.1016/j.surfcoat.2016.12.098.

Pulido-González N., García-Rodríguez S., Campo M., Rams J., Torres B., Application of DOE and ANOVA in Optimization of HVOF Spraying Parameters in the Development of New Ti Coatings. Journal of Thermal Spray Technology 29(3), 384-399, 2020. https://doi.org/10.1007/s11666-020-00989-9.

Riquelme A., Rodrigo P., An introduction on the laser cladding coatings on magnesium alloys. Metals 11(12), 1993, 2021. https://doi.org/10.3390/met11121993.

Rodríguez-Castro G. A., Reséndiz-Calderon C. D., Jiménez-Tinoco L. F., Meneses-Amador A., Gallardo-Hernández E. A., Campos-Silva I. E., Micro-abrasive wear resistance of CoB/Co2B coatings formed in CoCrMo alloy. Surface and Coatings Technology 284, 258-263, 2015. https://doi.org/10.1016/j.surfcoat.2015.06.081.

Tan Z. Q., Engström U., Li K., Liu Y., Effect of furnace atmosphere on sintering process of chromium-containing steel via powder metallurgy. Journal of Iron and Steel Research International 28(7), 889-900, 2021. https://doi.org/10.1007/s42243-020-00549-z.

Wang L., Zhang F., Yan S., Yu G., Chen J., He J., Yin F., Microstructure evolution and mechanical properties of atmosphere plasma sprayed AlCoCrFeNi high-entropy alloy coatings under post-annealing. Journal of Alloys and Compounds 872, 159607, 2021. https://doi.org/10.1016/j.jallcom.2021.159607.

Yu R. H., Basu S., Zhang Y., Xiao J. Q., Magnetic domains and coercivity in FeCo soft magnetic alloys. Journal of Applied Physics 85, 6034-6036, 1999. https://doi.org/10.1063/1.369073.

Zhang R., Lv K., Du Z., Chen W., Ji P., Wang M., Effects of Graphene on the Wear and Corrosion Resistance of Micro-Arc Oxidation Coating on a Titanium Alloy. Metals 12(1),70, 2022. https://doi.org/10.3390/met12010070.

Zhu Z. X., Liu X. B., Liu Y. F., Zhang S. Y., Meng Y., Zhou H. B., Zhang S. H., Effects of Cu/Si on the microstructure and tribological properties of FeCoCrNi high entropy alloy coating by laser cladding. Wear 512-513, 204533, 2023. https://doi.org/10.1016/j.wear.2022.204533.